Smart Structures and Systems, Vol. 5, No. 5 (2009) 517-529

DOI: http://dx.doi.org/10.12989/sss.2009.5.5.517

Adaptive tuned dynamic vibration absorbers working with MR elastomers

X. Z. Zhang and W. H. Li*

School of Mechanical, Materials and Mechatronic Engineering, University of Wollongong, Wollongong, NSW 2522, Australia

(Received October 29, 2007, Accepted June 6, 2008)

Abstract. This paper presents the development of a new Adaptive Tuned Dynamic Vibration Absorber (ATDVA) working with magnetorheological elastomers (MREs). The MRE materials were fabricated by mixing carbonyl iron particles with silicone rubber and cured under a strong magnetic field. An ATDVA prototype using MRE as an adaptable spring was designed and manufactured. The MRE ATDVA worked in a shear mode and the magnetic field was generated by a magnetic circuit and controlled through a DC power supply. The dynamic performances or the system transmissibility at various magnetic fields of the absorber were measured by using a vibration testing system. Experimental results indicated that this absorber can change its natural frequency from 35Hz to 90Hz, 150% of its basic natural frequency. A real time control logic is proposed to evaluate the control effect. The simulation results indicate that the control effect of MRE ATDVA can be improved significantly.

Keywords: tuned dynamic vibration absorber; magnetorheological elastomers; transmissibility; vibration control efficiency.

1. Introduction

Since their invention in 1900s, Tuned Dynamic Vibration Absorbers (TDVA) have been effectively used to suppress vibrations of machines and structures. The TDVA technology has found wide applications because it can offer high vibration reductions, good stability, low cost, low power and simplicity of implementation. Examples of such systems include machines, automobiles, aircrafts, generators, engines and motors, and building structures (Liu and Liu 2005, Lee, *et al*. 2001). However, the effectiveness of a conventional TDVA is always limited due to the narrow frequency ranges. In many practical applications, off-tuning of a TDVA occurs because of structural changes or varying usage patterns and loading conditions. To overcome these shortcomings, adaptive tuned dynamic vibration absorbers (ATDVAs) are extensively studied. The ATDVA is similar to the conventional TDVA but with adaptive elements that can be used to change the tuned condition. Commonly, adaptive stiffness elements are employed to vary the device natural frequency such that an ATDVA may be tuned to track uncertain or time-varying excitation frequencies.

Generally, ATDVA designs adopt two major groups: one is to use variable geometries and the other is to use smart or intelligent materials (Williams, *et al*. 2005). From the important view of system reliability and maintainability of ATDVA designs, Sun, *et al*. (1995) suggested the use of intelligent materials as

*Corresponding Author, E-mail: weihuali@uow.edu.au

alternatives. Davis and Lesieutre (2000) employed piezoelectric ceramic elements as part of the device stiffness, and reported the use of capacitive shunts to vary the device natural frequency from 290 Hz to 350 Hz. Williams, *et al*. (2005) used the thermal actuation of shape memory alloys (SMA) as tuning materials to develop an ATDVA. Testing showed that the SMA ATDVA natural frequency could be varied by approximately 15% from 38.5 Hz to 46.5 Hz. Though many attempts have been made, there are still some shortcomings, such as low responses, complex structures, prune to working conditions, etc.

Magnetorheological elastomers (MREs) are suspensions of magnetized particles dispersed in a polymer medium, such as rubbers. Magnetic Particles are mixed with a matrix. When individual particles are exposed to an applied magnetic field, magnetic dipole moments pointing along the magnetic field are induced in the particles. Pairs of particles then form head-to-tail chains. After the matrix is cured, the particles are locked into place and the chains are firmly embedded in the matrix. The elastic modulus of MREs increases steadily with the magnetic field increases. By removing the magnetic field, MR elastomers immediately reverse to their initial status. A number of research groups used this method to fabricate anisotropic MR elastomers (Ginder, *et al.* 2002, Bellan and Bossis 2002, Zhou 2004). A few groups reported the fabrication and testing of isotropic MR elastomers (Lokander and Stenberg 2003, Gong, *et al*. 2005).

The use of MREs to develop ATDVAs are expected to have many advantages: very fast response (less than a few milli seconds), simple structure, easy implementation, good maintenance, high stability, and effective control. Ginder, *et al.* (2002) did a pioneer work that utilized MREs as variable-spring-rate elements to develop an ADTVA. Their results indicated that a natural frequency ranged from 580 Hz to 710 Hz at a magnetic field 0.56 Tesla. However, the natural frequency varying was only 22% from its centre frequency. Deng, *et al*. (2006) developed MRE ATDVA whose natural frequency can be tuned from 55 to 82 Hz. Its absorption capacity was also experimentally justified. It is noted that a simple tuning method was used in their work. With this simple control strategy, it is very hard to achieve very good control effect, which greatly limited the advantages of MREs absorber.

Conventionally, tuning algorithm has been used for the absorber to track a single frequency disturbance on a primary system. This control logic was widely used because of the limitation of response time of conventional ATDVAs, which can provide relative lower damping factor, and their response time is not quick enough for promptly variation. However, this method is not fit for MRE ATDVA because of MREs' high level of damping inherent. Minimal damping is often recommended for an absorber, as excessive damping will limit the single-frequency attenuation greatly in exchange for expanded bandwidth. In addition, conventional absorbers can only control a single frequency excitation. When the disturbance force has several frequencies, it is very hard to identify which one of them is the dominant frequency and how to adjust the modulus of absorber. Because the tuning algorithm is so popular for semi-active TDVA control, the current MREs absorbers are using this control algorithm too, which greatly limit their control ability, such as suppression level and multi-frequency control. Although the multiple frequency excitations can be controlled by an active absorber, no prior study has been reported in the open literature that focuses on the multiple frequency control by using semi-active TDVA. This is the major motivation of this work. This paper aims to develop an MRE ATDVA and an effective control strategy, such that the system can take full advantage of the quick responses of MREs and also overcome the weak point of their high damping factors. For this purpose, silicone rubber based MR elastomers were fabricated and MRE ATDVA was manufactured and characterized. A new control logic is proposed to study the control efficiency. The simulation results indicate that the control effect of this novel absorber and control logic can be improved significantly. The multi frequencies disturbance can also be controlled effectively.

2. MRE samples

2.1. Fabrication of MREs

The Room Temperature Vulcanizing (RTV) silicon rubber (HB Fuller Company, Germany) and silicone oil were chosen as matrix. The volume fraction ratio of silicone oil and silicone rubber in the matrix is 1:1. The average diameter of carbonyl iron particle is about 5 μm (BASF Company, Germany). The carbonyl iron particles were immersed in the silicone oil, then they were mixed with RTV silicone rubbers. The mixture was put into a vacuum case to remove the air bubbles inside it, and then the mixture was poured into a mould. After being cured about 24 hour at the room temperature under a constant magnetic flux density 1 Tesla (electromagnetism system, Peking EXCEEDLAN Inc., China), MRE samples were prepared. Using this method, the MRE samples with particle volume fraction 30% were fabricated.

2.2. Characterization of MRE properties

The MR effect was evaluated by measuring the dynamic shear strain-stress curve of sample with and without an applied magnetic field using an Physica MRD 180 Magneto Rheolgical Device (Anton Paar Companies, Germany), equipped with an electromagnet kit. The rubber segments were approximately $\phi 20 \times 1$ mm, and they were sandwiched between a rotary disk and a base.

At a constant strain amplitude of 5% and a frequency of 1 Hz, relationships of shear stress against shear strain under various magnetic field strengths of 0, 125, 250, 375, and 500 mT, of MRE samples were measured and shown in Fig. 1. It can be seen from this figure that all curves show perfect elliptic hysteresis loops, which demonstrate the MREs behaves as linear viscoelastic properties. The loop areas increase steadily with the increase of magnetic fields, which demonstrates that the damping capabilities of MREs shows an increasing trend with magnetic field. Another interesting point is that the slop of the main loop axis shows an increasing trend with magnetic field. This demonstrates that the stiffness of MREs also increases steadily with magnetic field, which is totally different from MR fluids (Li and Du

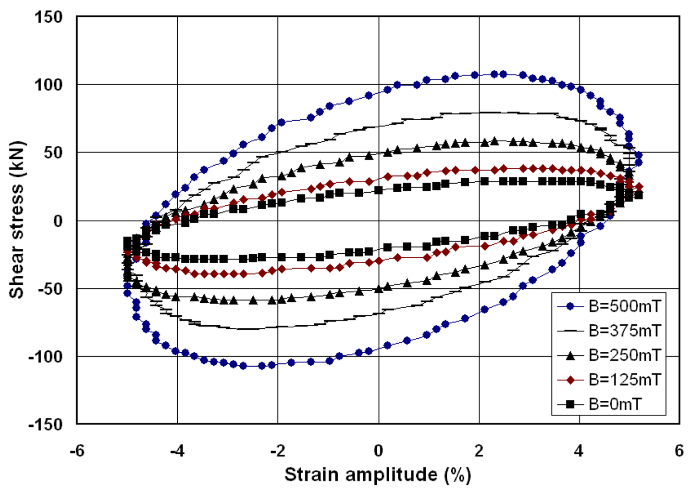

Fig. 1 Stress-strain hysteresis loop of MRE at different magnetic flux densities

2002, Li, *et al*. 2004). Therefore, MREs could be used as a novel Variable Stiffness Device for vibration control.

3. MRE ATDVA

3.1. Absorber's transmissibility

A dynamic vibration absorber can be looked as a single-degree-of-freedom (SDOF) vibration system. When the absorber was fixed on a vibration base, it can be looked as a simple SDOF system with foundation vibration stimulation. For this kind of system, when the displacement of the base is $x_b = a \sin\omega t$ (where a is the magnitude peak value of the displacement and ω is the vibration frequency), the differential equation of this system can be expressed as:

$$m\ddot{x} + c\dot{x} + kx = ka\sin\omega t + ca\omega\cos\omega t \tag{1}$$

where m is the mass of absorber, k is the stiffness of the spring, and c is damping coefficient.

The phase and magnitude of absorber's transmissibility were:

$$\phi = \tan^{-1}\frac{-2\zeta\lambda^3}{1-\lambda^2+(2\zeta\lambda)^2} \tag{2}$$

$$T = \sqrt{\frac{1+(2\zeta\lambda)^2}{(1-\lambda^2)^2+(2\zeta\lambda)^2}} \tag{3}$$

where $\omega_o = \sqrt{\frac{k}{m}}$, $\lambda = \frac{\omega}{\omega_0}$, $\zeta = \frac{c}{2m\omega_0}$. The frequency in which has the maximum value of T is the resonance frequency of the absorber, at the same time, the phase delay φ between the absorber mass and the base has the value $-\pi/2$. According to the Eqs. (2) and (3), if the mass of absorber is fixed on, the stiffness of the spring and the damping value can be worked out when the magnitude and phase of the absorber's transmissibility are obtained by experiments.

3.2. Experimental setup and implementation procedure

Conventionally, the absorbers can work in several modes: shear mode, flow mode and squeeze modes or other hybrid modes. The flow mode is not suitable for MR elastomers though some MR fluids based devices in this mode. The squeeze mode is not very suitable as the working ranges of MREs, such as displacement, are very narrow. Thus, the shear model is widely accepted to develop MRE absorbers. Additionally, the shear mode can provide better linear behavior in high shear strain. It is also convenient to compare different control effects of different program based on the developed shear mode MRE absorber. This project aims to develop a MRE absorber in shear mode. The device consisted of four basic components: an absorber mass, two MREs, an iron core and a coil of magnet wire. The dashed line shows the magnetic route (as shown in Fig. 2). The magnetic field is controlled by the electrical current intensity in the coil. The induced magnetic field is imposed in the direction of particles' chains in MREs and therefore it works in the shear mode. The magnetic flux density through the device was generated by creating a wire coil featuring N turns of wire carrying the current I in

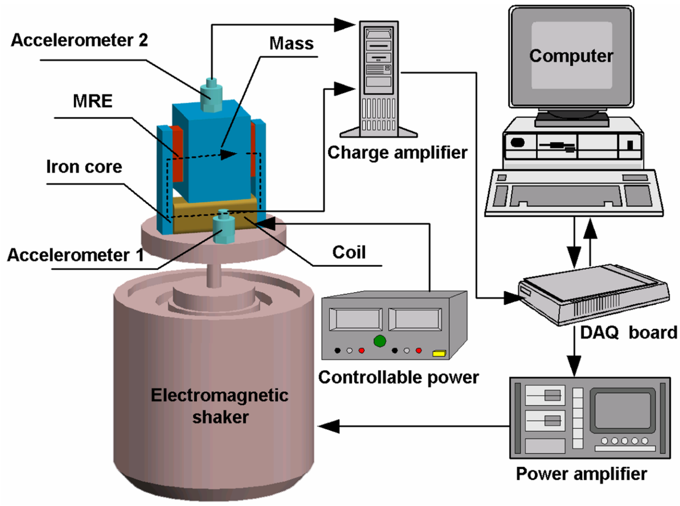

Fig. 2 The schematic of absorber testing

Amperes. The prototype has an absorber mass about 200 g and the turn number of the coil is 400. The diameter of wire is 1 mm. The coil resistance is 3 Ohm. The maximum current is 3A, so the maximum power consumption is about 27 watts. The thickness of the MREs is 6 mm and there were two pieces of MREs slices in the circuit. The effective pole area is 320 mm^2, and the section area of iron bar is 600 mm^2.

The schematic of the experimental setup is shown in Fig. 2. The absorber's base is fixed on an exciter, and it is the vibration foundation. The absorber is forced to vibrate by a vibration exciter (Type: JZK-5, SINOCERA PIEZOTRONICS, INC. China), which is driven by a signal source from a power amplifier (YE5871-100W) whose signal is provided by the Data Acquisition (DAQ) board (Type: LabVIEW PCI-6221, National Instruments Corporation. U.S.A) and computer. Accelerometer (Type: CA-YD-106) 1 and 2 monitor the vibrations of the base and the absorber mass. The signals are amplified by Charge amplifier (YE5851) and processed by DAQ and computer. A GW laboratory DC power supply (Type: GPR-3030D, TECPEL CO., LTD. Taiwan) can adjust the magnetic field intensity of the absorber and change its dynamic performance.

The testing interface designed in this system acts as the control unit and display unit for the ATDVA. The program is designed in LabVIEW (http://www.ni.com/labview/). The essential part of this system is the LabVIEW vibration package, which is used to generate the swept sine signals and to display and record the testing result for the property analysis of the TDVA. It can also be seamlessly connected to equipment PCI6221 DAQ board that are used as the interface between the computer and the amplifiers in this system. This program measures the frequency response of the device with a swept sine technique, generates a tone for the excitation signal and measures the magnitude and phase response of the device. The frequency response is measured at each test frequency, one frequency at a time. This testing program uses two analog input channels and one analog output channel. The start frequency and stop frequency determine the frequency range of the swept-sine measurement. The sample rate is 2.5 times the value of the maximum of the two frequencies. Fig. 3 shows a typical result of the transmissibility and phase versus sweeping frequency. In this experiment, the start frequency is chosen as 0 Hz and the stop frequency is 200 Hz. The number of steps is set as 50, which determines the total number of test frequencies. This result verified that the absorber is a SDOF system as there is only one

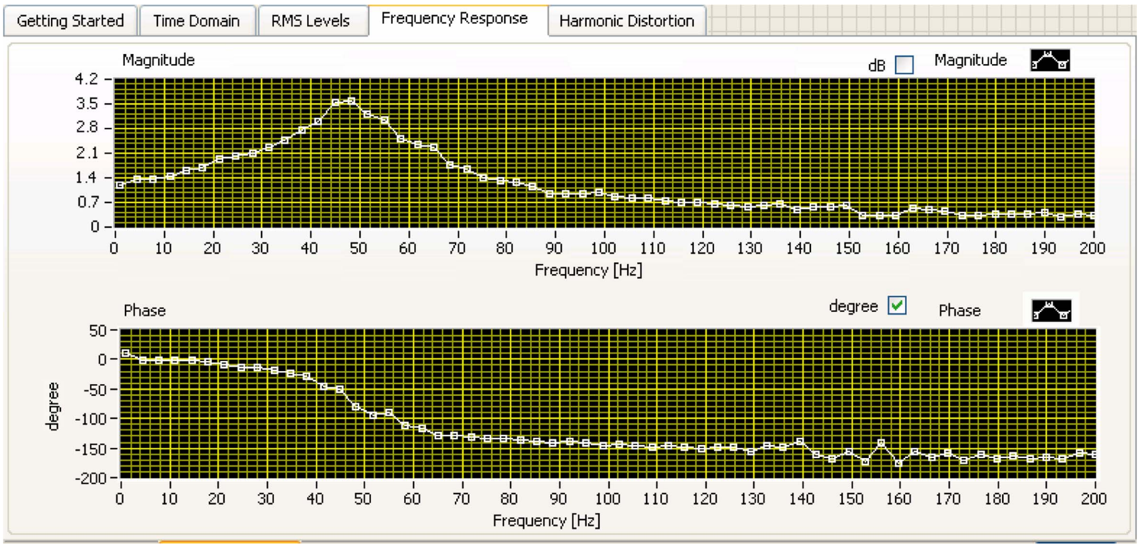

Fig. 3 The interface of LabVIEW and a typical experiment result

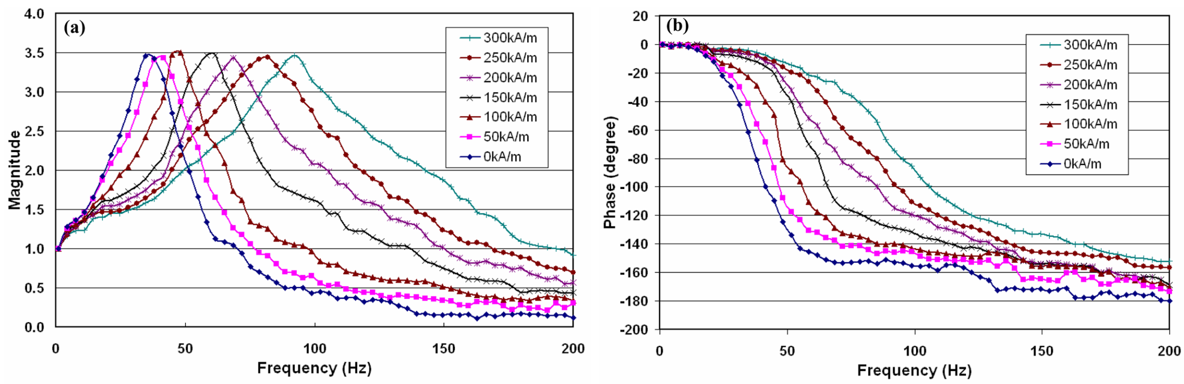

Fig. 4 Transmissibility and phase of the absorber in different magnetic field intensity. (a) transmissibility versus frequency for various field intensities; (b) phase versus frequency for various field intensities

peak amplitude in the frequency range. Five different magnetic fields of 0, 50, 100, 150, 200, 250 and 300kA/m have been used in this experiment. The current intensity in the coil are ranged from 0 to 3A (The maximum current intensity which the power supply can provide). Because the stiffness is depended on the MREs field-depended modulus as $k = GA/t$ (G is the shear modulus, A and t are the section area and thickness of MREs sample, respectively), the different magnetic field can adjust the stiffness of the absorber.

Fig. 4(a) and (b) show the transmissibility and phase of the absorber at various magnetic fields. As can be seen from these figures, the natural frequency of absorber increases from 35 Hz at without current intensity to 90 Hz when the control current intensity is 3A. The control bandwidth of ATDVA is related to the rate of relative change of natural frequency. And this absorber has about 150% relative frequency change.

For each magnetic field, substitute the transmissibility value at natural frequency $\omega = \omega_n$ into Eq. (3). The damping ratio can be calculated using $\zeta = \dfrac{1}{2\sqrt{T^2 - 1}}$. The stiffness of the absorber at each magnetic field can be calculated using the equation $k = m\omega_n^2$. According to the experimental results, the stiffness increase steadily with the increment of magnetic field/current intensity. Their relationships can be expressed as

$$k = 0.517H^2 + 37.381H + 9742.5 \ (\mathrm{N/m})$$

$$\text{and } k = 5169.9I^2 + 3738.1I + 9742.5 \ (\mathrm{N/m}) \tag{4}$$

The unit of magnetic field H is kA/m in the equation. However, the damping ratio varies very little with the magnetic field, so it can be considered as a constant value 0.15.

4. Vibration suppression verification

An analysis about the ATDVA was given in this section. A new control algorithm was given.

4.1. Steady state frequency response characteristics of vibration absorber

As shown in Fig. 5, the structure of the systems can be modeled by the linear springs k and k_a, the damping factors c and c_a, the masses m and m_a. k is the stiffness of suspension spring of primary system and k_a is the stiffness of MREs. The MREs stiffness k_a can be changed with the magnetic field applied on the ATDVA. m is the sprung mass and m_a is the moving mass of ATDVA. $F(t)$ are the forces on mass. The parameters of the absorber were obtained by experimental results.

The damping is quantified by c and c_a, denoting the primary system and absorber system damping, respectively. The governing equations of this system are

$$\begin{bmatrix} m & 0 \\ 0 & m_a \end{bmatrix}\begin{bmatrix} \ddot{x}(t) \\ \ddot{x}_a(t) \end{bmatrix} + \begin{bmatrix} c + c_a & -c_a \\ -c_a & c_a \end{bmatrix}\begin{bmatrix} \dot{x}(t) \\ \dot{x}_a(t) \end{bmatrix} + \begin{bmatrix} k + k_a & -k_a \\ -k_a & k_a \end{bmatrix}\begin{bmatrix} x(t) \\ x_a(t) \end{bmatrix} = \begin{bmatrix} F \\ 0 \end{bmatrix} e^{j\omega t} \tag{5}$$

Inman (2001) presents a metric called the "normalized magnitude". This defines a ratio of the primary mass amplitude divided by the static displacement that would be caused by a constant force of equivalent magnitude. By defining several other non-dimensionalized parameters, the entire equation can be non-dimensionalized:

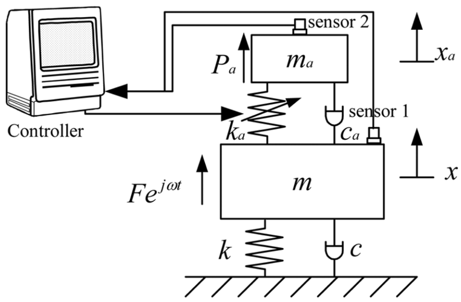

Fig. 5 Schematic of the MRE ATDVA system

$\mu = \frac{m_a}{m}$ (Mass ratio)

$\omega_a = \sqrt{\frac{k_a}{m_a}}$ (The term ω_a refers to the natural frequency of the absorber, which is also a resonance frequency. This is the fundamental concept behind the tuned vibration absorber)

$\omega_p = \sqrt{\frac{k}{m}}$ (Natural frequency of primary system without absorber)

$\beta = \frac{\omega_a}{\omega_p}$ (Ratio of system natural frequencie)

$r = \frac{\omega}{\omega_p}$ (Ratio of excitation frequency to primary system natural frequency)

$\varsigma_p = \frac{c}{2m\omega_p}$ (Damping ratio of primary system)

$\varsigma_a = \frac{c_a}{2m_a\omega_a}$ (Damping ratio of absorber system)

Using these definitions, the normalized magnitude can be found to be

$$\left|\frac{Xk}{F}\right| = \sqrt{\frac{(r^2-\beta^2)^2 + 4\varsigma_a^2 r^2\beta^2}{[(r^2-1)(r^2-\beta^2) - \mu r^2 - 4\varsigma_a\varsigma_p r^2]^2 + \{2\varsigma_a r\beta[1-(1+\mu)r^2] + 2\varsigma_p r(r^2-\beta^2)\}^2}} \tag{6}$$

Illustrated in Fig. 6 is a typical frequency response of the primary system and the composite system including a dynamic absorber. The amplitude values are the normalized magnitude of primary system.

When an absorber with a natural frequency $\omega_a = \omega_p$ is attached to the system, the single resonance peak of the primary system is replaced by two resonances on either side of the original resonance; the

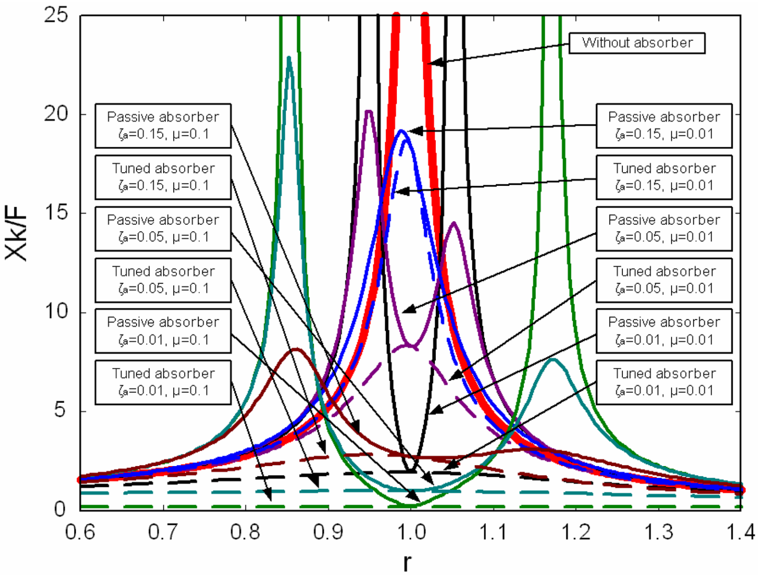

Fig. 6 Frequency response of the primary system

original resonance has now been replaced by anti-resonance. If excitation is provided by machinery operating near the natural frequency, vibration can be reduced by attaching the absorber so that anti-resonance is created near that frequency. This is the principle of passive absorber. The greater the mass ratio, the further apart the resonance frequencies will be. With damping present, the level of attenuation is less at the resonance frequency but the range over which attenuation in the vibration response is provided is now increased. A semi-active absorber can always work in tuned condition, in Fig. 6, the dash line shows that the two new resonant frequencies induced by absorber can be avoided too. For smaller values of mass ratio, the sensitivity of the absorber to tuning increases. For example, when the mass ratio is 0.1, the semi-active absorber with high damping ratio 0.15 can also achieve a much better control effect than a passive absorber. But when the mass ratio is 0.01, the semi-active absorber with high damping ratio does not have any notable advantage compared with passive absorber.

According to the figure, the absorber with high mass ratio and low damping ratio can achieve a better control effect. However, as a redundant mass, it is expected that the absorber mass ought to be as less as possible. The conventional "tuned control" is fit for the absorber with metal adaptable spring, such as SMA, which has relative low damping ratio and low response. But it can not take full advantage of the quick response of MRE absorber and overcome the weak point of its high damping factor. These results are well-known to researchers, but there were very few methods which can overcome these weak points of conventional dynamic vibration absorber. This is one of the major motivations of this article. Therefore, the primary aim in next research is to design an optimal control strategy for MRE absorber.

4.2. Control algorithm for MRE absorber

The Eq. (5) representing the system can be transferred into

$$M\ddot{X} + C\dot{X} + KX = L_C u + L_S f \tag{7}$$

where f is the force from the vibrating source and u is the control force applied to the system. M, C, and K are mass, damping coefficient and stiffness matrices respectively. X is the state variable matrix. $L_C = [-1, 1]^T$ and $L_C = [1, 0]^T$ are the parameters of the control force and excitation force, respectively.

The following state equation is obtained from Eq. (7):

$$\dot{Z} = AZ + Bu + Df \tag{8}$$

where $Z = [X\ \dot{X}]^T$, $A = \begin{bmatrix} 0 & I \\ -M^{-1}K & -M^{-1}C \end{bmatrix}$, $B = \begin{bmatrix} 0 \\ M^{-1}L_C \end{bmatrix}$ and $D = \begin{bmatrix} 0 \\ M^{-1}L_S \end{bmatrix}$.

I is one identical matrix.

Now, define the Lyapunov function candidate

$$V = Z^T P Z \tag{9}$$

where P is the positive definite solution of Lyapunov equation

$$PA + A^T P + Q = 0 \tag{10}$$

for a given symmetric positive definite matrix Q. The matrix Q can be selected as $Q = \eta P$, because P is positive definite matrix and η is the coefficient to P. By using Eqs. (7)-(10), the derivative of V(x, t) is obtained

$$\dot{V} = -\eta V + (B^T uPZ + Z^T PBu + D^T fPZ + Z^T PDf) \tag{11}$$

The external applied forces include the excitation force as well as the control force. The control objective is to keep $\dot{V} < 0$ and minimize $\dot{V}$.

In this case, the control force can be written as

$$u(t) = \Delta k_a (x - x_a) \tag{12}$$

where Δk_a is the increment of MRE's stiffness due to magnetic field.

To exploit the full capabilities of the actuators, bang-bang control was used in this paper. The key characteristic of optimal bang-bang control is a control force that switches from one extreme to another (Wu and Soong 1996). The controller is designed to compensate (or reduce) to the extent achievable, for the reduction of the system response. One possible controller is obtained by minimizing $\dot{V}$ in Eq. (11). It is expressed as

$$u(t) = g(t)\Delta k_{ai}(x - x_a) \quad \text{and} \quad g(t) = \begin{cases} 0 & (x - x_a)\dot{x} \le 0 \\ 1 & (x - x_a)\dot{x} > 0 \end{cases} \tag{13}$$

Where $g(t)$ is one switch function, showing the values of 0 and 1. Δk_{ai} is the stiffness increment of MRE spring.

According to Eqs. (4) and (13), we chose a real time controller. The current intensity in coil is controlled by the controller

$$i(t) = \begin{cases} 1 & [x_1(t) - x_2(t)]x_1(t) > 0 \\ 0 & [x_1(t) - x_2(t)]x_1(t) \le 0 \end{cases} \quad \text{and} \quad K_a(t) = \begin{cases} 4000(N/m) & [x_1(t) - x_2(t)]x_1(t) > 0 \\ 1200(N/m) & [x_1(t) - x_2(t)]x_1(t) \le 0 \end{cases} \tag{14}$$

where $i(t)$ is the control signal in real time. When $i(t) = 1$, the power is switched on and the control current intensity is 2A. The current intensity is 0.4A when $i(t) = 0$.

The control effects of the absorbers are simulated by simulink in MATLAB. The parameters in the simulation are based on the experimental results. The stiffness modification is according to Eq. (4), and the mechanical parameters are the same as the prototype's described in 3.2. At first, an excitation force is applied to excite the system, which is a sine sweeping waves with amplitude 1 from 1 to 200 Hz during 200s, and the response forces on m with different control logics are compared and shown in Figs. 7(a) and (b). In Fig. 7(a), the mass ratio of absorber and primary system is 0.1. This ratio is 0.01 in Fig. 7(b). The natural frequency of primary system was set as 60 Hz.

The response force on m without control is shown in Fig. 7. The primary system without control has high response when the excitation-signal nears its natural frequency. At the tuned frequency it is noted that the system with passive absorber have an anti-resonance point. This leads to minimum displacement and therefore the minimum energy enters the primary system. The absorber provided shifted resonant frequencies that are outside the disturbance frequency near the natural frequency of primary system. It can also be found that the suppression effect is decreased much with low mass ratio when we compare Fig. 7(a) with Fig. 7(b).

A semi-active absorber worked in tuned condition can avoid two new resonant frequencies induced by TDVA, but in low mass ratio, it does not have any notable advantage compared with passive absorber. The high damping ratio decreased the level of attenuation at the resonance frequency, but provided the absorber a robust and fail-safe behaviour, for the response is not high even in off tuned condition.

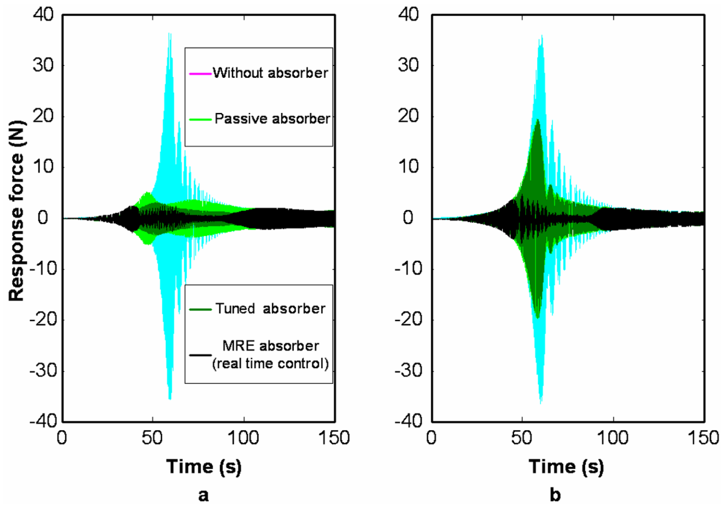

Fig. 7 Response signals of the system. (a) mass ratio is 0.1; (b) mass ratio is 0.01

Fig. 7 shows the force on *m* with MRE ATDVA by using the optimal real time control logic. In high mass ratio, this control logic has almost the same effect as that of "tuned" control logic. In addition, this control logic has a perfect control effect even the mass ratio is only 0.01, while the conventional "tuned" control logic almost has no effect then. It proved that the level of attenuation at the resonance frequency can also be very high even in high damping ratio and low mass ratio if a proper control logic was used. The advantage of fail-safe behaviour is also kept in MRE ATDVA.

Then, to verify the capability of MRE ATDVA to control the multi-disturbance, an excitation force composed of five signals is applied on the system. It has one sine sweeping waves with amplitude 1 from 1 to 200 Hz and the other one from 35 to 90 Hz during 200s, three sine waves with amplitude 1

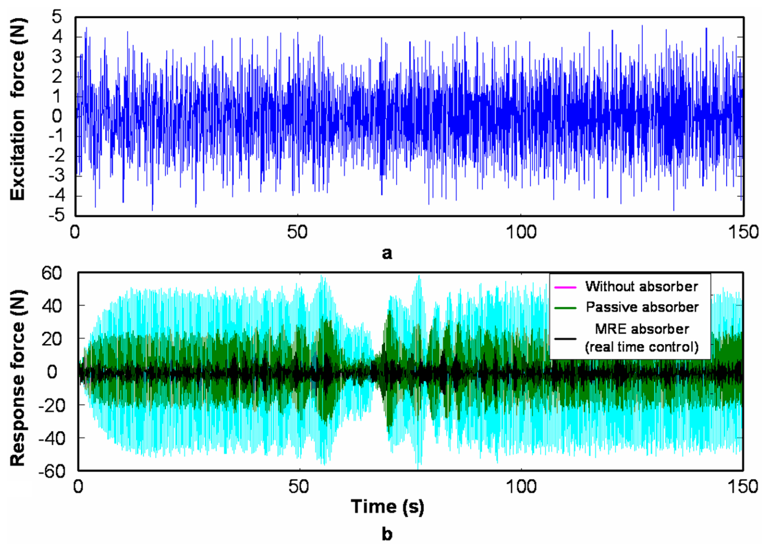

Fig. 8 Excitation and response signals of the system (mass ratio 0.01). (a) Excitation signal; (b) Comparison of primary system responses

and constant frequencies of 35, 50 and 90 Hz, respectively (The excitation force is shown in Fig. 8(a)). For conventional tuned dynamic vibration absorber, it is very hard to identify which one is the dominant frequency and how to adjust the absorber to fit for the dominant frequency. It can only be used as a passive TDVA. But MRE absorber with real time control can deal with this case without problem. Fig. 8(b) shows the control effect of the absorber. It gives the response forces on *m* without control, with a passive TDVA and with a MRE ATDVA by using real time control logic. The mass ratio in this simulation is 0.01. According to the results, the system without control has large force amplitude because the excitation signals are closed to its natural frequency. A passive TDVA can suppress the amplitude of the primary system to about half value. While the MRE ATDVA using real time control logic can suppress the vibration of primary system obviously. It is clear that the force amplitude of controlled system is lower than that of the passive system in any time, i.e. the controlled MRE ATDVA has a much better control effect even in very low mass ratio.

5. Conclusion

In this paper, the MREs based on silicone rubber and carbonyl iron particles were fabricated. The dynamic performances of MREs samples in different magnetic field were tested by a rheological testing system.

A semiactive dynamic vibration absorber using MREs as adaptable spring was designed and manufactured. This MRE ATDVA worked in shear mode and the magnetic field was controlled by a coil and a controllable DC power. The controllable dynamic behaviours of the absorber were also tested by a vibration testing system. Experimental results indicated that this absorber can change its natural frequency from 35 Hz to 90 Hz, 150% of its basic natural frequency.

A simulation to evaluate the vibration reduce efficiency was given. The parameters of the model are calculated according to the experimental results. Numerical simulation results indicate that the proposed semi-active absorber can trace the disturbance force frequency and absorb the inertial energy transferred from the primary structure and suppress the vibration of primary system.

To take full advantage of the quick response of MRE ATDVA and overcome the weak point of its high damping factor, a novel real time control logic has been presented to minimize the vibration amplitude of the system. This controller and quick response of MRE ATDVA can provide the system real time control ability. Numerical simulation results indicate that the proposed MRE ATDVA and control logic have many notable advantages: 1. Compare with passive absorber, it can produce much better performance; 2. Compare with classical tuned absorber, its level of attenuation at the resonance frequency can also be very high even in high damping ratio and low mass ratio. In addition, it can control the system with multi-excitation force; 3. The MREs' high level of damping inherent provided a robust and fail-safe behaviour to the absorber.

References

Bellan, C. and Bossis, G. (2002), "Field dependence of viscoelastic properties of MR elastomers", *Int. J. Mod. Phys. B,* **16**(17&18), 2447-2453.

Davis, C.L. and Lesieutre, G.A. (2000), "An actively tuned solid-state vibration absorber using capacitive shunting of piezoelectric stiffness", *J. Sound Vib.,* **232**(3), 601-617.

Deng, H.X., Gong, X.L. and Wang, L.H. (2006), "Development of an adaptive tuned vibration absorber with

magnetorheological elastomer", *Smart Mater. Struct.,* **15**(5), N111-N116.
Ginder, J.M., Clark, S.M., Schlotter, W.F. and Nichols, M.E. (2002), "Magnetostrictive phenomena in magnetorheological elastomers", *Int. J. Mod. Phys. B,* **16**(17&18), 2412-2418.
Gong, X.L., Zhang, X.Z. and Zhang, P.Q. (2005), "Fabrication and characterization of isotropic magnetorheological elastomers", *Polym. Test*., **24**(3), 324-329.
Lee, E.C., Nian, C.Y. and Tarng, Y.S. (2001), "Design of a dynamic vibration absorber against vibrations in turning operations", *J. Mater. Process. Tech.,* **108**, 278-285.
Li, W.H. and Du, H. (2002), "Nonlinear rheological behavior of magnetorheological fluids: step-strain experiments", *Smart Mater. Struct.,* **11**, 209-217.
Li, W.H., Du, H. and Guo, N.Q. (2004), "Dynamic behavior of MR suspensions at moderate flux densities", *Mater. Sci. Eng. A*, **371**, 9-15.
Liu, K. and Liu, J. (2005), "The damped dynamic vibration absorbers: revisited and new result", *J. Sound Vib.,* **284**, 1181-1189.
Liu, K. and Liu, J. (2005), "The damped dynamic vibration absorbers: revisited and new result", *J. Sound Vib.,* **284**, 1181-1189.
Lokander, M. and Stenberg, B. (2003), "Performance of isotropic magnetorheological rubber materials", *Polym. Test*., **22**(3), 245-251.
Sun, J.Q., Jolly, M.R. and Norris, M.A. (1995), "Passive, adaptive, and active tuned vibration absorbers-a survey", *J. Mech. Design,* **117B**, 234-242.
Williams, K.A., Chiu, G.T.C. and Bernhard, R.J. (2005), "Dynamic modelling of a shape memory alloy adaptive tuned vibration absorber", *J. Sound Vib.,* **280**, 211-234.
Wu, Z. and Soong, T.T. (1996), "Modified bang-bang control law for structural control implementation", *J. Eng. Mech.* ASCE, **122**(8), 771-777.
Zhou, G.Y. (2004), "Complex shear modulus of a magnetorheological elastomer", *Smart Mater. Struct.,* **13**, 1203-1210.

JM